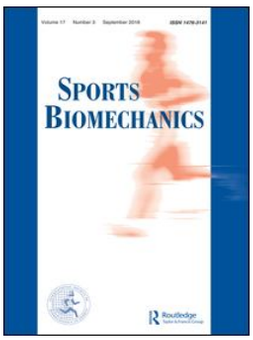

Sports Biomechanics

ISSN: 1476-3141 (Print) 1752-6116 (Online) Journal homepage: http://www.tandfonline.com/loi/rspb20

Validation of a videogrammetry technique for analysing American football helmet kinematics

Ann Bailey, James Funk, David Lessley, Chris Sherwood, Jeff Crandall, William Neale & Nathan Rose

To cite this article: Ann Bailey, James Funk, David Lessley, Chris Sherwood, Jeff Crandall, William Neale & Nathan Rose (2018): Validation of a videogrammetry technique for analysing American football helmet kinematics, Sports Biomechanics, DOI: 10.1080/14763141.2018.1513059

To link to this article: https://doi.org/10.1080/14763141.2018.1513059

Published online: 02 Oct 2018.

SPORTS BIOMECHANICS
https://doi.org/10.1080/14763141.2018.1513059

Routledge
Taylor & Francis Group

ARTICLE

Validation of a videogrammetry technique for analysing American football helmet kinematics

Ann Bailey[a], James Funk[a], David Lessley[a], Chris Sherwood[a], Jeff Crandall[a], William Neale[b] and Nathan Rose[b]

[a]Biomechanics Consulting and Research, Charlottesville, VA, USA; [b]Kineticorp, Greenwood Village, CO, USA

ABSTRACT

Professional American football games are recorded in digital video with multiple cameras, often at high resolution and high frame rates. The purpose of this study was to evaluate the accuracy of a videogrammetry technique to calculate translational and rotational helmet velocity before, during and after a helmet impact. In total, 10 football impacts were staged in a National Football League (NFL) stadium by propelling helmeted 50th percentile male crash test dummies into each other or the ground at speeds and orientations representative of concussive impacts for NFL players. The tests were recorded by experienced sports film crews to obtain video coverage and quality typically available for NFL games. A videogrammetry procedure was used to track the position and rotation of the helmet throughout the relevant time interval of the head impact. Compared with rigidly mounted retro-reflective marker three dimensional (3-D) motion tracking that was concurrently collected in the experiments, videogrammetry accurately calculated changes in translational and rotational velocity of the helmet using high frame rate (two cameras at 240 Hz) video (7% and 15% error, respectively). Low frame rate (2 cameras at 60 Hz) video was adequate for calculating pre-impact translational velocity but not for calculating the translational or rotational velocity change of the helmet during impact.

ARTICLE HISTORY
Received 5 April 2018
Accepted 9 August 2018

KEYWORDS
Injury biomechanics; rotational kinematics; head; model-based image matching

Introduction

The design of American football (henceforth, football) safety equipment requires an understanding of the loading conditions that are experienced by players on-field. There are two general methods that have been used to quantify the severity of head impacts in football: sensors and videogrammetry. Various sensor packages have been developed for the mouth guard and helmet to quantify head kinematics during an impact (Camarillo, Shull, Mattson, Shultz, & Garza, 2013; Rowson et al., 2011; Rowson & Duma, 2013). Sensors are a promising approach because they can provide direct measurements of head motion during all impacts sustained by a player, both injurious and non-injurious. However, current systems have documented issues with accuracy under certain impact conditions (Jadischke, Viano, Dau, King, & McCarthy, 2013; Siegmund, Guskiewicz,

CONTACT Ann Bailey abailey@biocorellc.com

Marshall, DeMarco, & Bonin, 2016), and there are no published reports of sensor data from football at the professional level.

At present, given the high quality of video available for National Football League (NFL) games, the biomechanics of on-field concussive head impacts in the NFL can be determined most accurately using videogrammetry, which is the science of taking three-dimensional (3-D) measurements from two-dimensional (2-D) video images. Previously, NFL game video from 31 on-field impacts was analysed to calculate the velocities, positions and closing speed of the colliding players just before impact (Pellman, Viano, Tucker, Casson, & Waeckerle, 2003). In this previous study, the motion of the helmets during and after impact was not quantified from video. Rather, the kinematics of the head during the time of impact were reconstructed physically by propelling helmeted partial crash test dummies at each other in the measured pre-impact configuration, then quantifying the impact severity based on sensor measurements from the dummies' heads. Based on validation experiments, it was estimated that the error in the video-estimated closing speed between colliding heads could be as high as 11%, and the compounding error of the physical reconstruction process could lead to errors as high as 17% for peak resultant translational head acceleration and 25% for peak resultant rotational head acceleration (Newman, Beusenberg, Shewchenko, Withnall, & Fournier, 2005). Videogrammetry has also been used to calculate the closing velocity between the head and its collision partner during concussive head impacts in the helmetless sports of rugby and Australian football (McIntosh, McCrory, & Comerford, 2000). Validation work in that study indicated that the error in the video-derived closing velocities was below 10%. As far as we are aware, all previous works on video analysis of naturalistic, on-field sports concussions have been limited to measurements of pre-impact closing velocity (McIntosh et al., 2000; Oeur, Karton, Post, Rousseau, Hoshizaki, Marshall, Brien, Smith, Cusimano, Gilchrist, 2015; Pellman et al., 2003). In the last few decades, notable improvements have been made to the quality of videography in terms of frame rate and resolution. Furthermore, advances in photogrammetric theory and model-based image-matching (MBIM) techniques have increased video analysis capabilities and accuracy (Koga et al., 2010; Tierney et al., 2017). Given these advancements, we felt that an attempt to directly and accurately measure the kinematics of the helmet before, during and after impact using videogrammetry was warranted. Direct measurement of the helmet kinematics during an impact pulse from video is complementary or even preferable to indirect methods that make estimates of the head kinematics during impact based on pre-impact conditions.

The purpose of this study is to document the accuracy of a video analysis technique applied to measuring helmet velocities in football in terms of quality of the available broadcast video (view angles, image resolution and frame rate). Specifically, helmet kinematic data were collected from staged on-field helmet-to-helmet and helmet-to-ground impacts using videogrammetry, helmet instrumentation and an optically based 3-D motion capture system using retroreflective markers. Errors in the videogrammetry methodology were quantified by comparing results to the 3-D motion capture system, which was considered the baseline standard for measuring helmet motion. Errors were calculated for pre- and post-impact, peak and change in translational and rotational velocities of the helmet. It was hypothesised that while videogrammetry may be used to

accurately measure initial conditions for an impact, the measured change in translational and rotational velocity during the impact may be less accurate, with accuracy being correlated with video frame rate.

Methods

On-field impact testing

Helmeted crash test dummies were propelled into each other in an NFL stadium (Lucas Oil Stadium in Indianapolis, IN, USA) to simulate generalised on-field helmet impact configurations representative of those encountered by players during NFL games. The anthropomorphic test devices (ATDs) were partial Hybrid III 50th percentile male crash test dummies instrumented with 6DX-Pro sensors (Diversified Technical Systems, Seal Beach, CA, USA) in the head, torso and rigidly mounted to the interior of the helmet shell. Upper and lower neck load cells (mg-sesnor, Rheinmuenster, Germany) were also used. The ATDs included a head, neck, torso and pedestrian pelvis. No upper and lower extremities were included out of concern that their effect on head kinematics would be minimal and unrealistic. The launch system (Figure 1) was composed of two identical electric-powered belt-driven sleds, which could be fired separately at speeds up to 8 m/s. The ATDs were mounted to each sled at two points. The weight of the dummy was primarily supported by a metal eye hole connector attached to a climbing harness that was adjusted to fit the torso of the dummy. The dummy was initially hung on the sled by sliding the eye hole connector over a short forward-facing horizontal post on the launching frame of the sled. Next, the bottom of the dummy was connected to the launch frame using a custom-made modification to the pedestrian pelvis. The connection consisted of a door latch that slid into a slot in the launch frame. The door latch was loosely attached to a metal piece on the bottom of the

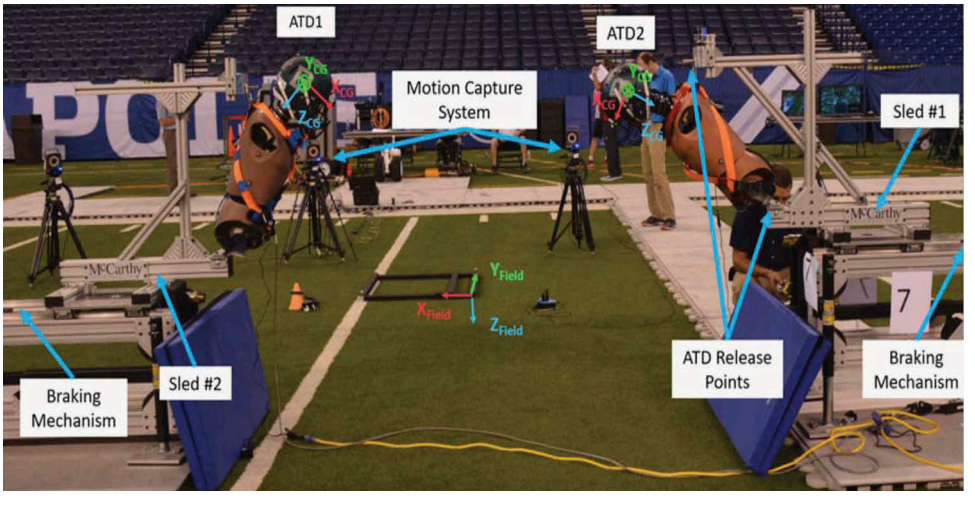

Figure 1. Electrically driven sled system used for on-field impact testing. global (field) and local (CG) coordinate systems are shown. the local helmet coordinate system was initially aligned with the head coordinate system with its origin at the centre of gravity of the hybrid III head.

pelvis that was bolted to the hip sockets. The location of the upper eye hole mount could be changed by adjusting the arms of the launching frame, thereby allowing a range of different torso angles at launch. The dummies were launched by accelerating the sleds up to the desired velocity, then rapidly decelerating the sleds at the end of their track. When the sled decelerated, the eye hole and slot connectors slid out of place and the dummies were cleanly released.

In total, 10 impact configurations were created to represent generalised on-field helmet-to-helmet and helmet-to-ground impact scenarios. Impact locations were established from a qualitative review of videos from concussive impacts in the NFL, and closing velocities for the impacts were within the range of those calculated from a video analysis performed by Pellman et al. (2003). The test configurations included centred and eccentric impacts in front, side, rear and oblique directions at speeds up to 8 m/s (Figure 2). Configurations 1–3 were helmet-to-ground impacts, whereas configurations

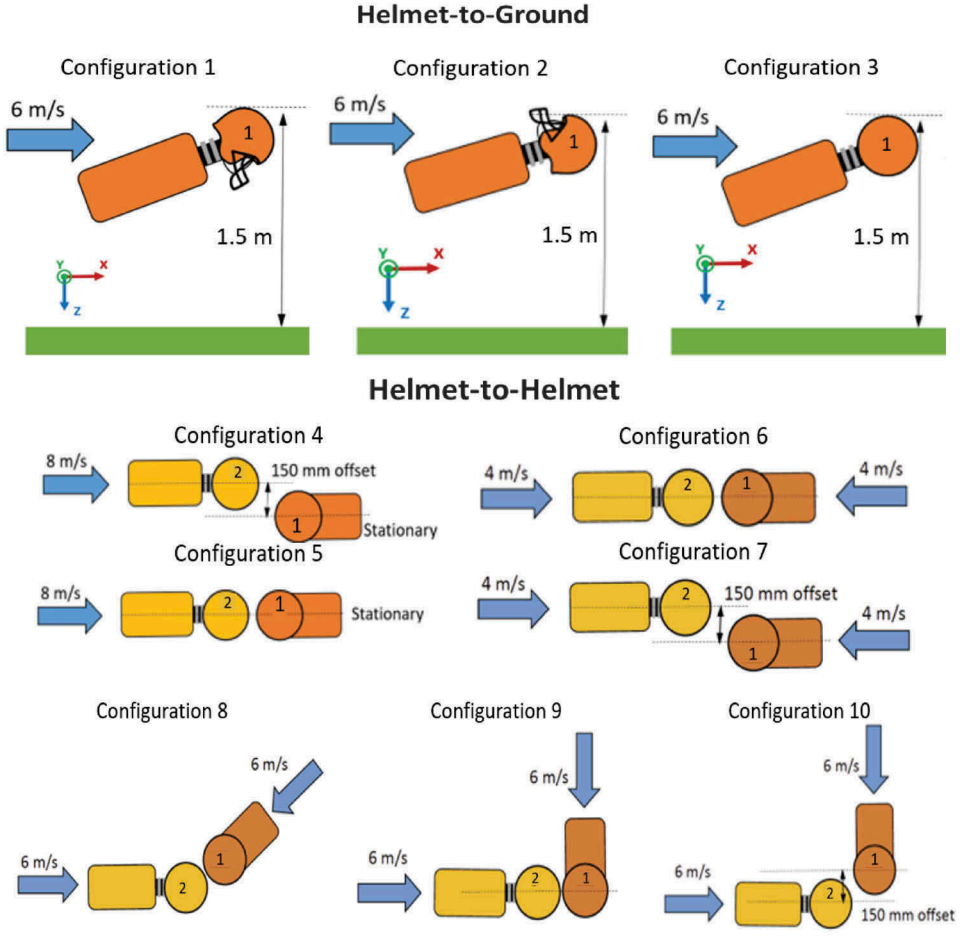

Figure 2. Impact configurations for simulated on-field helmet-to-helmet and helmet-to-ground dummy impacts. ATD1 and ATD2 are labelled along with pre-impact velocities.

4–10 were helmet-to-helmet impacts. Configurations 4 and 5 involved one moving dummy striking one stationary dummy, whereas configurations 6 and 7 involved two moving dummies striking each other. Configurations 4 and 6 were meant to be identical in terms of relative speeds but different in terms of absolute speeds, as were configurations 5 and 7. In practice, the launch trajectories varied slightly from run to run, so the impact dynamics were not identical in these pairs of tests. The ground impacts were simulated by launching the dummy horizontally with its head slightly above its pelvis so that the ground impact with the torso induced a whipping motion of the head into the ground. For initial positioning, torso elevation angles were measured using digital inclinometers to document the angle of the Hybrid III spine box relative to the ground. For configurations 1–3, the spine box of ATD1 was positioned 30° from horizontal. For the remaining configurations, ATD1 and ATD2 were positioned with spine box angles of 60° and 30° relative to horizontal, respectively.

A Riddell Revolution® Speed Classic (R41179, Riddell, Elyria, OH, USA) helmet was placed on ATD 1, whereas a Schutt Air XP Pro (789,102, Schutt, Litchfield, IL, USA) was placed on ATD 2. Both helmets were size large which is the most appropriate size for the 50th percentile Hybrid III head (Jadischke et al., 2013). Nylon stockings were placed over the heads of the dummies to reduce the friction between the vinyl skin of the Hybrid III and the inside of the helmets (Jadischke, Viano, McCarthy, & King, 2016; Viano, Withnall, & Halstead, 2012). Helmets were positioned on the head form by aligning the helmet centre with the head form nose in the x-y plane, and then rotating the helmet in the x-z plane until there was a 75 mm distance between the helmet brim and the bottom of the nose (National Operating Committee on Standards for Athletic Equipment [NOCSAE] (2015); Rowson et al., 2011).

Motion capture

Helmet kinematics were captured at 1000 Hz using an optoelectronic stereo-videogrammetric motion capture system (Vicon™, Los Angeles, CA, USA) consisting of 18 near-infrared cameras closely positioned around the impact area. The motion capture software tracked the trajectories of spherical retroreflective markers through a calibrated 3-D space within the cameras' collective field of view. Multiple markers were rigidly attached to the shell of each helmet used in the tests, while additional markers were rigidly attached to a stationary reference frame aligned with the playing field. Virtual models of the helmet were created using data from 3-D optical scans of the helmet (Faro Focus, FARO®, Lake Mary, FL, USA). A 3-D coordinate system was established for each helmet that was defined to be initially coincident with the standard 3-D coordinate frame of the dummy's head as defined by SAE J211 (Society of Automotive Engineers, 1995). To relate the position of the helmet to the head, the positions of various landmarks on the helmet, head and neck were collected using a Romer Absolute Arm-6Axis (Exact Metrology, Cincinnati, OH, USA) while the helmet was properly positioned on the dummy head. The position and orientation of the helmet at each point in time were determined by automatically matching the virtual helmet model to the measured helmet marker locations using a previously developed optimisation technique (Lessley, Shaw, Riley, Forman, & Crandall, 2011). Transformation matrices were calculated to relate the helmet coordinate system to

the fixed field coordinate system at each time point. Based on a previous error analysis (Lessley et al., 2011), we estimate that the motion capture data were able to locate the position of the helmet with an error of less than 1 mm in this study. Therefore, the motion capture data were considered the gold standard, and errors in the videogrammetric analysis were calculated with respect to the motion capture data.

Videography

Game-style video was recorded by professional film crews (IMS Productions, Indianapolis, IN and NFL Films, Mount Laurel Township, NJ, USA) to replicate the type of video footage typically collected during NFL games, including camera panning and zooming. In total, 11 cameras were placed in seven standard locations for game coverage (Figure 3 and Table 1). Multiple cameras with different frame rates were placed side by side in some locations, and two of the cameras were carried by operators on the sideline. To simulate typical panning and zooming characteristics, a play was simulated by having a researcher receive the snap and run in a sweeping motion towards the sled. The sled was manually fired as the ball carrier reached the sled. The video operators were instructed to smoothly pan and zoom to follow the ball carrier and transition to the dummy on the sled as they would follow a play in a game situation.

It is important to note that much broadcast video, including that collected in this study, is interlaced. In interlaced video, each frame consists of two fields (even and odd

Figure 3. Location of cameras used for filming each impact event. camera locations were numbered, and cameras designated with an 'A' indicate a second camera at a higher frame rate at that location.

Table 1. List of camera locations (in field coordinates) and their respective frame rates. Note that cameras 8 and 10 were mobile so locations are listed as variable.

Camera ID	Frame Rate (images/s)	X (m)	Y (m)	Z (m)
1	60	13.42	70.16	−48.50
1A	240	13.42	70.16	−48.50
2	60	13.09	55.56	−21.87
2A	240	13.09	55.56	−21.87
4	60	−43.04	−20.26	−31.36
4A	240	−43.04	−20.26	−31.36
6	60	115.57	30.27	−16.71
7	30	13.09	55.56	−21.87
8	120		variable	
9	120	−1.13	8.36	−1.61
10	120		variable	

rows of pixels in the image) that are recorded at twice the frame rate. Each field contains half of the image data in a full frame. Standard video editing software is capable of de-interlacing the video so that each field can be accessed and analysed separately. The image collection rate in interlaced video is really the field rate, which is twice as high as the frame rate (e.g., 30 frames/s interlaced video is equivalent to 60 fields/s). For the sake of brevity, we will use the term 'frame rate' in this paper to mean image collection rate, and all quantifications of frame rate will be in terms of the number of images (fields) recorded per second.

Videogrammetry

Camera view selection

The first step in the videogrammetry process was selecting camera views to analyse. The amount and quality of camera coverage in an NFL game can vary widely depending on game date, venue and other factors. Most stadiums have similar locations for cameras, but the resolution and frame rate of the cameras vary widely. Our goal was to select the best camera views for analysis that would be representative of NFL game video. At least two camera views with sufficient angular separation were required to triangulate the position of the helmet. Each view had to show the object of interest (the helmet) throughout the relevant time frame. Other factors that affected the quality of the video were object resolution and edge definition. Object resolution was defined as the helmet's size within the image in terms of the number of pixels spanning the diameter of the helmet (pixels per helmet). Edge definition was subjectively assessed based on qualities such as brightness, contrast and presence of blur. Based on these factors, it was determined that the cameras at locations 2 and 4 provided the best footage for analysis. These were standard high-level views from the side at the 50-yard line and the centre of the end zone that are available in all games (Figure 3). The angle of separation between these camera views was 96° for the location on the field where the impact experiments were conducted. In some cases, the video analysis was supplemented with a sideline view from camera 9. The angle of separation between cameras 9 and 4 was 66°. The distance between the camera and the impact area was approximately 74 m for location 2, 100 m for location 4 and 20 m for location 9.

To establish appropriate frame rates for analysis in this study, a survey of available game video footage from 84 concussion cases from the 2015–2016 season was

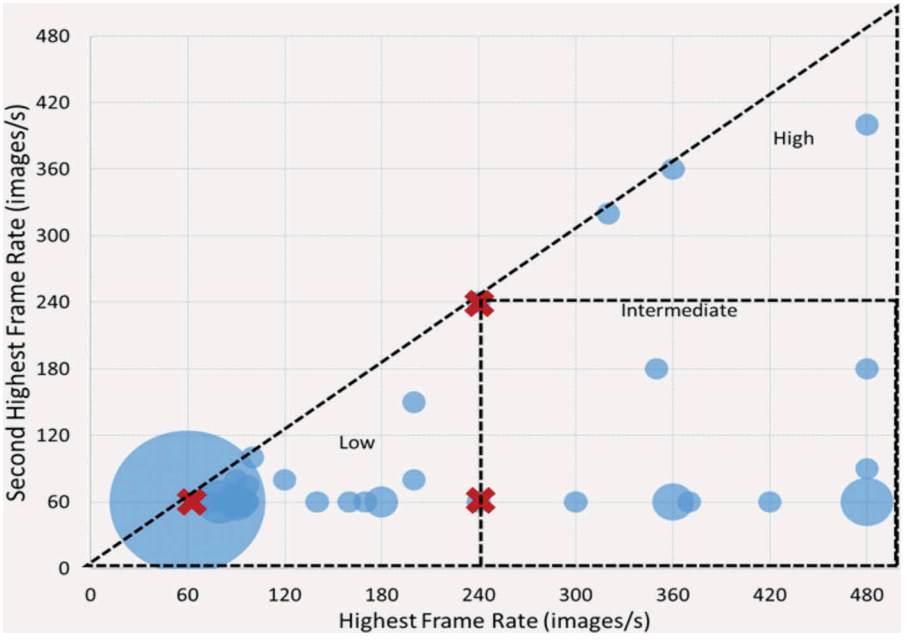

Figure 4. Summary of catalogued videos for concussion events from the 2015-2016 NFL season, where the radius is proportional to the number of data points with a particular combination of frame rates. frame rate scenarios used in the analysis are indicated by an 'x'.

conducted. These 84 cases were felt to be generally representative of available game video. The best two views for video analysis were chosen (but not analysed) for each case based on frame rate and video quality. The cases were then arranged in a bubble plot (in which the radius of the bubble is proportional to the number of cases) based on the highest and second-highest frame rates of the two selected views (Figure 4). From these data, we defined three levels of video quality based on the number of available camera views with a frame rate of 240 images/s or greater: 0 = *low* (49% of cases), 1 = *intermediate* (41% of cases) and 2 = *high* (10% of cases).

Three combinations of frame rates were chosen for this validation study to represent the low, intermediate and high end of frame rates available in NFL game video (Table 2). The low frame rate scenario was represented by analysis of two camera views recorded at 60 images/s (cameras 2 and 4). The intermediate-frame rate scenario was represented by an analysis of one camera view recorded at 240 images/s (camera 2A) and one camera view recorded at 60 images/s (camera 4). The high-frame rate scenario was represented by an analysis of two camera views recorded at 240 images/s (cameras 2A and 4A), sometimes supplemented with a sideline camera with a frame rate of 240 images/s. These analyses were performed using video footage taken from side-by-side cameras to isolate the effect of frame rate on the video analysis. The goal of this study was to estimate the error associated with various combinations of frame rates and establish the level of video quality (in terms of frame rate) necessary for the videogrammetry methodology to yield acceptably accurate results.

Table 2. Matrix of camera views and resolution in pixels per helmet used to perform the validation study for each test configuration and for each frame rate scenario.

Frame Rates	Low 60–60 images/s		Intermediate 240–60 images/s		High 240–240 images/s	
Test #	Views	Resolution (pixels/helmet)	Views	Resolution (pixels/helmet)	Views	Resolution (pixels/helmet)
1	2, 4	3526, 1385	2A, 4	5153, 1385	2A, 4A	5153, 1590
2	2, 4	4301, 1075	2A, 4	2922, 1075	2A, 4A	2922, 3217
3	2, 4	5809, 707	2A, 4	5675, 707	2A, 4A, 9	5675, 1075, 18,627
4	2, 4	5809, 1195	2A, 4	3739, 1195	2A, 4A	3739, 661
5	2, 4	4072, 661	2A, 4	4657, 661	2A, 4A, 9	4657, 1134, 13,893
6	2, 4	4301, 1195	2A, 4	4778, 1195	2A, 4A, 9	4778, 1662, 8825
7	2, 4	9331, 5675	2A, 4	4657, 1195	2A, 4A	4657, 3019
8	2, 4	5675, 755	2A, 4	4657, 755	2A, 4A, 9	4657, 1590, 16,513
9	2, 4	3739, 1257	2A, 4	3848, 1257	2A, 4A, 9	3848, 1257, 16,061
10	2, 4	3632, 2206	2A, 4	2252, 2206	2A, 4A	2552, 1590

Note: Resolution is provided in pixels per area of the helmet for each camera view

Video processing

All camera views were 'stabilised' to remove the effects of camera movement, panning, tilting and zooming so that the background shown in each image remained stationary (Nuke X 10.0v1, Foundry, London, UK) (Figure 5(a)). This procedure simplified the tracking process by reducing the number of variables the tracking software needed to evaluate.

Computer software was used to calculate each camera's position, orientation and field of view through a technique called camera matching (3ds Max 2018, PF-Track 2015.1.1, Pixel Farm, Kent, UK). A virtual model of the field at Lucas Oil Stadium was created from a 3-D laser scan of the field and stadium interior (Faro Focus X330, FARO®, Lake Mary, FL, USA). A virtual view of this model was created for each camera, and the position, angle and zoom of each camera were determined by manually adjusting these virtual settings until the field markings matched up in superimposed virtual and video views. The effects of lens distortion were incorporated into the virtual view based on the lens profile of each camera (Neale, Hessel, & Terpstra, 2011). The accuracy of this method was assessed by comparing the position of each camera calculated by the camera-matching technique to the actual position of each camera measured in the laser scan of the stadium.

Helmet tracking

The position and orientation of the helmet in all six degrees of freedom was determined at each time point using a model-based image-matching (MBIM) technique. A two-step process was used to streamline the analysis. First, a circular outline, the same size as the helmet was manually fit around the outline of the helmet at each time point in each camera view (Figure 5(b)). With the path of the helmet tracked in two dimensions from different vantage points, the position of the helmet in the 3-D environment (the field and stadium) was then determined using ray-tracing from the two known camera locations (Side FX Houdini™ 15.5.763) (Neale, Hessel, & Koch, 2016). A ray was emitted from each camera and projected through the 2-D tracked paths. The position at which the rays from different cameras intersected was the approximate position of the helmet's geometric centre in each frame of the footage.

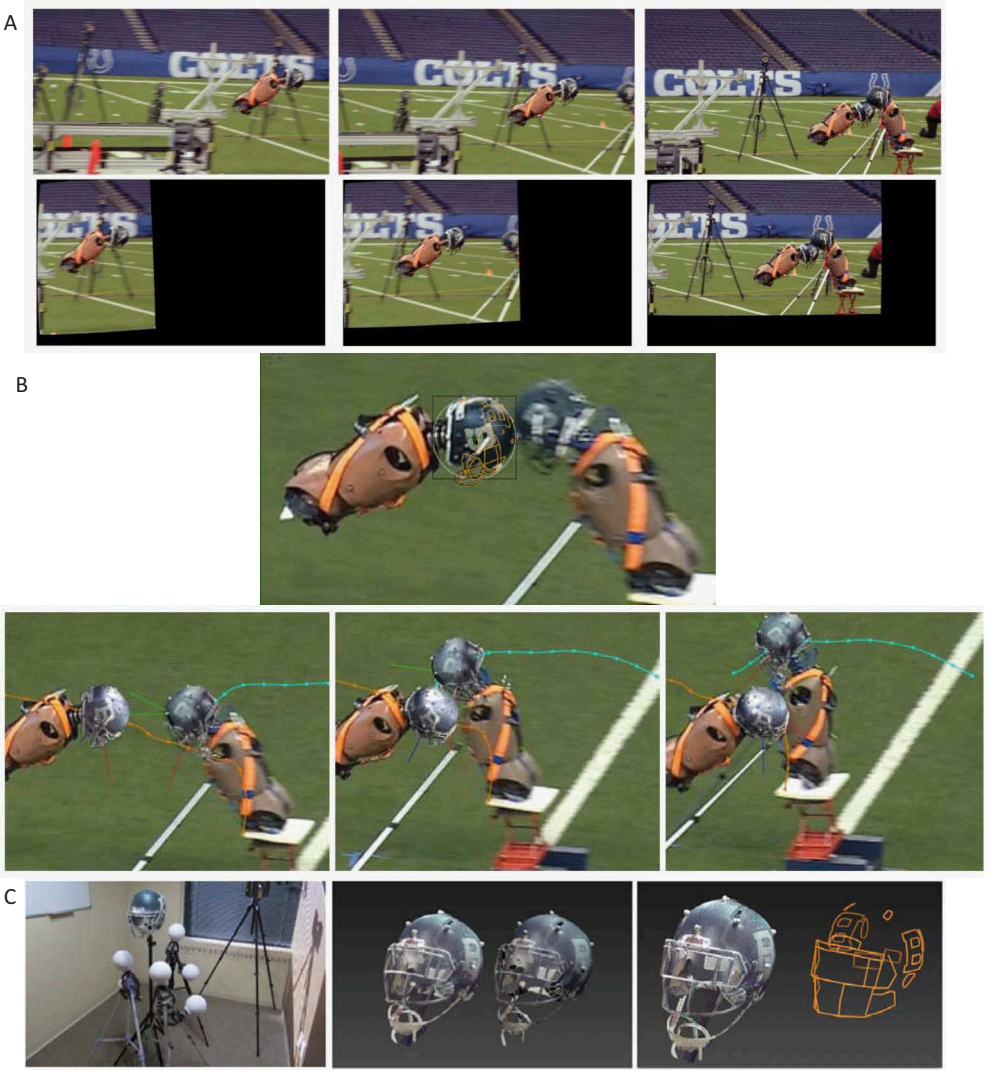

Figure 5. (A) Demonstration of the effect of stabilisation. the top row of images shows original images, while the bottom row shows post-processed stabilised images. note how the background in the top row moves from the right to the left in the frame, whereas the background for the bottom row remains stationary in the frame. (B) A trace of the helmet generated from the 3-D scan data was used to track helmet position in two dimensions (top). Computer-modelled helmet-matching was then used to acquire rotational position data using the 2-D translational positions as a starting point (bottom). (C) process for obtaining helmet geometry, consisting of 3-D scanning, creating a 3-D computer model, and generating a 3-D trace of helmet features.

Having defined the approximate 3-D path of the helmet, the precise location and rotation of the helmet was determined by model-based image-matching. A stripped-down model of the helmet was created for videogrammetry from the optical scan data. The videogrammetric model included 3-D traces of the facemask, logo and other helmet landmarks. The retroreflective markers were explicitly excluded from the videogrammetric

helmet model (Figure 5(b)). At each time point, the 3-D position and rotation of the helmet were determined by manually adjusting all six degrees of freedom until the helmet markings matched up in superimposed virtual and video views (Houdini™, Side Effects Software, Toronto, Canada; 3ds Max®, Autodesk, San Rafael, CA, USA) (Figure 5(c)). Kinematic data were exported in the form of a directional cosine matrix relating the local helmet coordinate frame to the global field coordinate frame.

Data processing

After the video analysis, a study was performed to investigate the effect of different filtering techniques on the error between the motion capture and videogrammetric kinematic data. Since the data were collected at different sampling rates (1000 Hz for motion capture and 60–240 Hz for the video analysis), different filtering cut-off frequencies were required for each set of data. The same filtering algorithm was used in all cases (forward and reverse, 4-pole Butterworth filter). A Fast Fourier Transform (FFT) was performed on the ATD head sensor data to establish the range of relevant frequencies. The normalised amplitude of the FFT for linear acceleration was less than 10% for frequencies exceeding 200 Hz, which was consistent with a study by Wu, Zarnescu, Nangia, Cam, and Camarillo (2014) that studied the bandwidth requirement for helmet sensors. For rotational velocity, normalised amplitudes of the FFT were less than 10% for frequencies greater than 50 Hz. These thresholds were used to establish the cut-off frequencies for the motion capture data. Translational position data from the motion capture system were filtered to 50 Hz. The filtered translational position data were differentiated using a standard two-point symmetric finite difference method and then filtered to 100 Hz to obtain translational velocity. Rotational velocity data were calculated from the direction cosine matrices and filtered to 50 Hz. Filter cut-off frequencies for the videogrammetry-derived kinematics were selected so as to minimise error when compared to the motion capture data. To establish cut-off frequencies for the videogrammetry-derived kinematics, 4-pole Butterworth filters at 10 Hz cut-off frequency intervals were applied, and the data traces were compared with the filtered motion capture data. The filter cut-off frequency which produced the least error for each ATD from each test was recorded. The most common filter cut-off frequencies associated with minimum error for each measure are reported in Table 4. A cut-off frequency of 50 Hz was selected for all stages of processing of the high and intermediate frame rate videogrammetry data, and a 30 Hz cut-off frequency was selected for all stages of processing of the low frame rate data.

The time-varying six degree of freedom kinematic data were reduced to several key parameters that became the subject of the error analysis. These parameters were pre-impact resultant translational velocity (V_0), pre-impact resultant rotational velocity (ω_0), pre-impact heading angle, change in translational velocity (ΔV), change in rotational velocity ($\Delta\omega$), maximum resultant translational velocity (V_{max}), maximum resultant rotational velocity (ω_{max}) and post-impact heading angle (Table 7 and 8). Pre-impact velocities were calculated as the average velocity over a 5 ms time window prior to first helmet contact (for helmet-to-helmet configurations 4–10) or first body contact with the ground (for helmet-to-ground configurations 1–3) as determined from video. Because calculating velocity from position data at different sample rates affects the timing of the

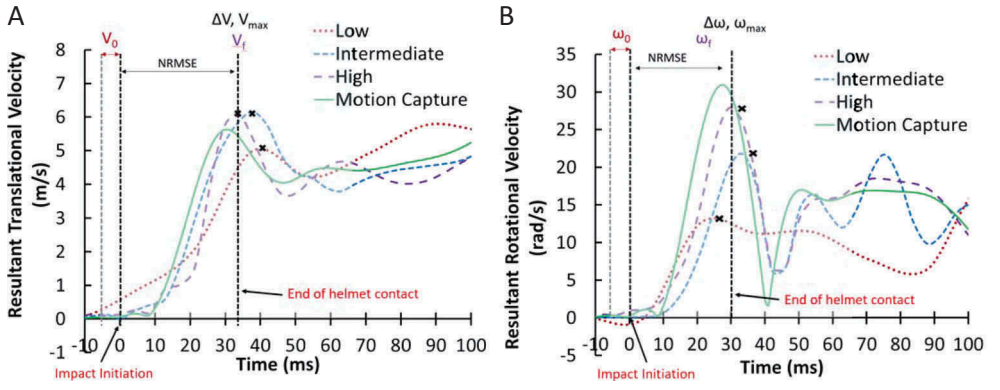

Figure 6. Example of data processing for ATD1 for test 5 showing the time ranges used to calculate NRMSE, change in velocity, and maximum velocity for translational velocity (A) and rotational velocity (B). note that impact initiation was time of body contact with the ground for configurations 1–3 and helmet contact for configurations 4–10. Time of maximum ΔV and Δω are indicated by 'x's for each frame rate scenario.

transient helmet response, the time range over which maximum helmet velocity (V_{max} and ω_{max}) and change in helmet velocity (ΔV and Δω) were evaluated was extended to encompass 50 ms beyond the end of helmet contact as determined from the video (grey areas on Figure 6).

Error analysis

The accuracy of the videogrammetry was quantified by calculating the error in each parameter with respect to the motion capture data, which were considered the baseline (gold standard). Mean errors were calculated using absolute values of the error so that offsetting errors would not cancel out. Kinematic parameters were compared not just at individual time points but also over the time history of the impact. The latter comparisons were accomplished by calculating the root mean square error (RMSE), normalised root mean square error (NRMSE) and correlation and analysis (CORA) between the videogrammetric and motion capture data over the entire impact time window (Gehre, Gades, & Wernicke, 2009). Total CORA scores were calculated using equal weighting of size, phase and progression scores.

Linear regression analysis was used to establish a base level of validity for evaluation of low, intermediate and high frame rate video. The analysis of videogrammetric versus motion capture data was performed for six kinematics parameters: pre-impact translational velocity (V_0), pre-impact rotational velocity (ω_0), change in translational velocity (ΔV), change in rotational velocity (Δω), maximum resultant translational velocity (V_{max}) and maximum resultant rotational velocity (ω_{max}). If a Student's *t*-test determined that the slope of the regression line was significantly different from one, or the intercept was statistically different from zero, at the $\alpha = 0.05$ level, then the videogrammetry data in that regression were considered invalid (Siegmund et al., 2016).

Results

The accuracy of the camera-matching method was assessed by comparing the calculated position of each camera to the actual position of each camera measured using the laser scan of the stadium. Error in location estimates ranged from 5 to 30 cm, which amounted to less than 1% error when considering the distance of the cameras from the on-field impact locations (76–100 m). Videogrammetry was very accurate when measuring pre-impact helmet velocity, with absolute errors of less than 0.4 m/s and 0.9 rad/s for initial resultant translational and rotational velocity, respectively, at all frame rates studied (Figure 7). Average error in pre-impact position was 0.08 ± 0.10 m for the high and intermediate frame rate results, although some of this error may have been due to the process of time-syncing the motion capture data with the videogrammetry data. Further, the error for translational and rotational velocity was found to be consistent for all directional components for each frame rate scenario. Videogrammetric measurements of helmet heading angle were also very accurate, especially for the initial heading angle, where all errors were less than 5°. The errors in the videogrammetric measurements of final velocity, change in velocity, and peak velocity were all similar. In each case, substituting higher frame rate video for lower frame rate video substantially reduced the error in the videogrammetry. If one camera view had high frame rate footage (240 images/s), then the change in translational helmet velocity could be measured with an overall error of 0.4 m/s (9%) and the change in rotational helmet velocity could be measured with an overall error of 3 rad/s (17%) (Figure 8(a)). The NRMSE calculated over the entire time window of impact was 19% for resultant translational velocity and 15% for resultant rotational velocity (Figure 8(b)). For intermediate frame rates, total CORA scores ranged from 0.90 to 0.99 and 0.75 to 0.99 for resultant translational velocity and resultant rotational velocity, respectively (Figure 8(c)).

The linear regression analysis showed that all helmet velocity parameters measured by videogrammetry passed the validity test (they were not statistically different from the motion capture data) if at least one camera view was available with high frame rate footage (240 images/s) (Table 3). In videogrammetric analyses using only low frame footage (60 images/s), the only kinematic parameters that did not fail the validity test were initial translational helmet velocity and change in rotational helmet velocity (Table 5).

Discussion and implications

The accuracy of videogrammetry for tracking helmet motion is dependent on many variables, including the frame rate and resolution of individual cameras, the location of the players on the field, their speed and direction of travel, the angle between the cameras and the degree of view obstruction. A full exploration of all of these variables was not feasible for this study. We chose to evaluate the accuracy of our particular implementation of videogrammetry using footage that was as realistic as possible. The test matrix included a wide range of impact speeds and configurations that were generally representative of concussive impacts that occur in NFL games (Pellman et al., 2003).

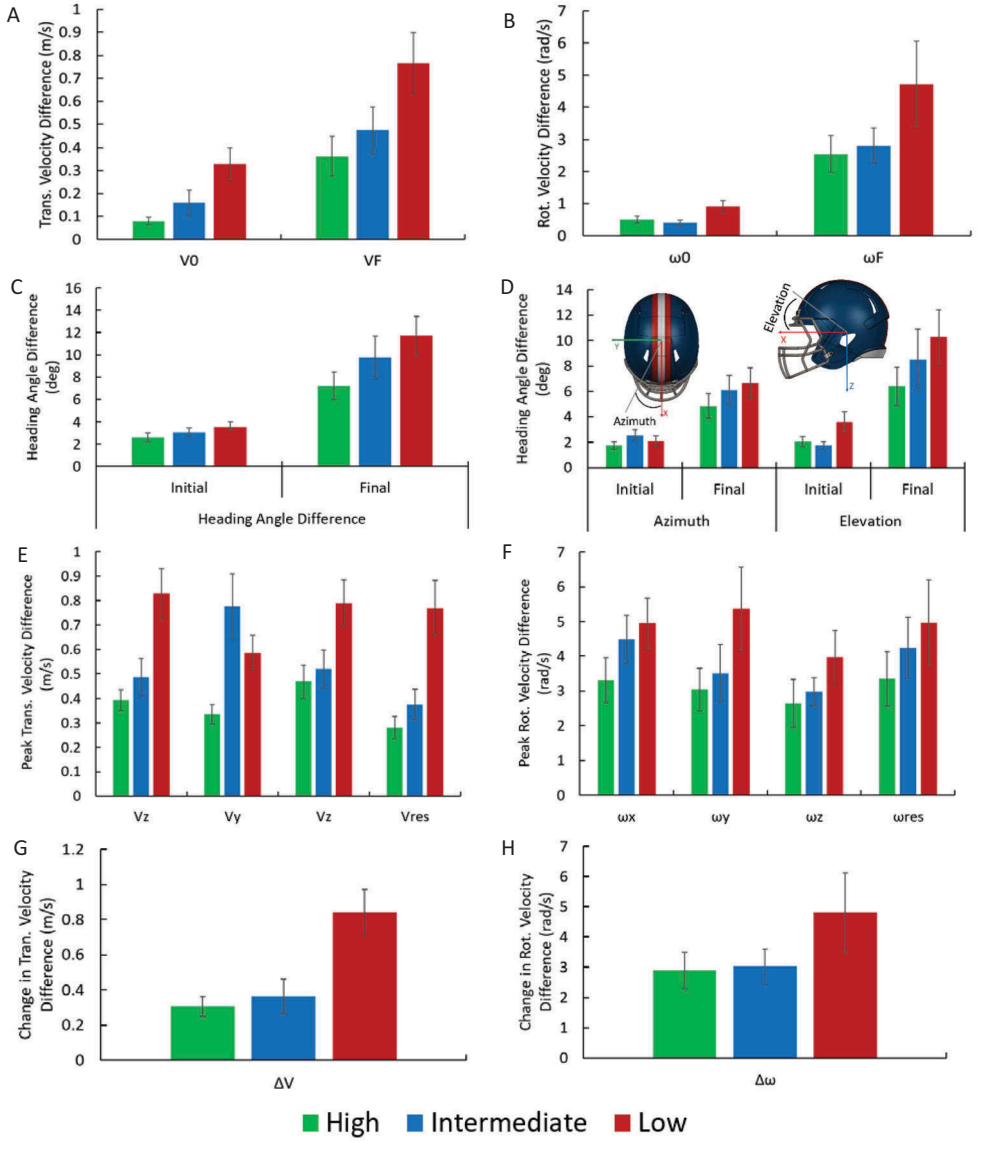

Figure 7. Average absolute error (and standard error) for all helmets in all 10 test configurations. (A) shows the error for the resultant initial and final resultant translational velocity, (B) shows the error for the initial and final resultant rotational velocity in the helmet coordinate system, (C) shows the initial and final global translational velocity heading angle differences, (D) shows the difference in azimuth and elevation components of initial and final global translational velocity, and (E) and (F) show the difference in peak translational and rotational velocities. (G) and (H) show the error associated with the change in translational and rotational velocities.

Our analysis indicates that using video with lower frame rates leads to less accuracy for capturing peaks and changes in translational and rotational velocities (Figures 7 and 8). Errors for the high and intermediate frame rate scenarios tended to be similar, whereas errors were significantly higher for the low case compared with the high and intermediate

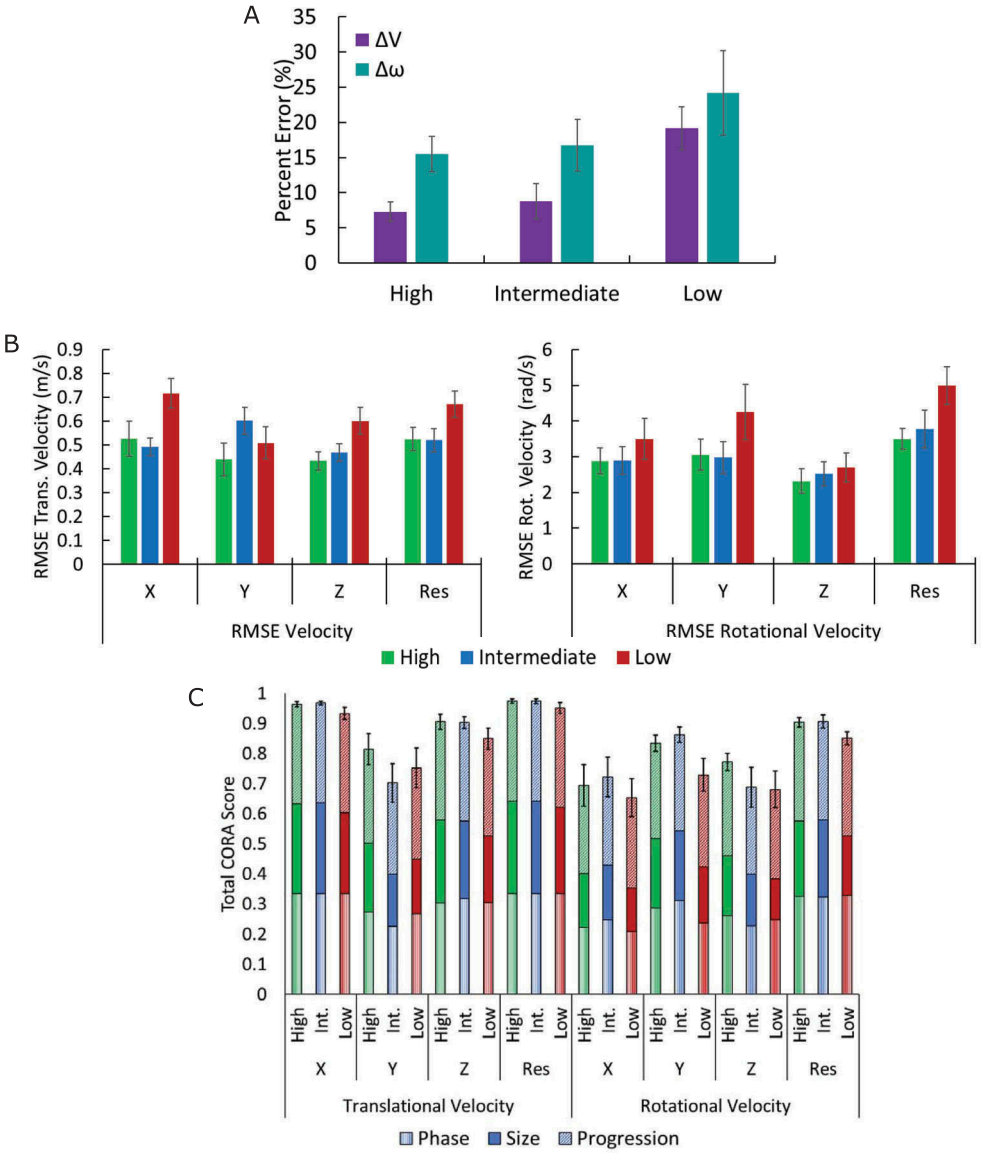

Figure 8. (A) Comparison of average percentage error for change in translational and rotational velocity and for all three frame rate scenarios. error bars represent the standard error. (B) comparison of average root mean squared error (RMSE) for all test configurations for translational (left) and rotational (right) velocity and for all three frame rate scenarios. (C) comparison of total correlation and Analysis (CORA) scores for resultant and components of translational and rotational velocity. the three parts of the CORA score are represented by patterns, and error bars represent the standard error for the total score.

cases (see Table 6). The low frame rate video (60 images/s) was inadequate for measuring anything but the pre-impact translational velocity of the helmet (Table 4) due to underestimation of sudden velocity changes (Figures 9, 10, and 11). However, if video footage from at least one camera was captured at a frame rate of 240 images/s or greater, videogrammetry

Table 3. Summary of validation testing. videogrammetric measurements passed the validation test if they were not significantly different from the motion capture data in a linear regression.

Kinematic Parameter	High Frame Rate	Intermediate Frame Rate	Low Frame Rate
Peak V	Yes	Yes	No
Peak ω	Yes	Yes	No
ΔV	Yes	Yes	No
Δω	Yes	Yes	Yes
V_0	Yes	Yes	Yes
ω_0	Yes	Yes	No

Table 4. Most common filter cut-off frequency associated with the largest error reduction for each kinematic measure for each of the 10 test configurations.

	240 fps, 240 fps		240 fps, 60 fps		60 fps, 60 fps	
Measurement	Translational	Rotational	Translational	Rotational	Translational	Rotational
Initial Velocity Magnitude	50 Hz	50 Hz	50 Hz	50 Hz	30 Hz	30 Hz
Initial Velocity Heading	50 Hz	-	50 Hz	-	15 Hz	-
Final Velocity Magnitude	30 Hz	30 Hz	20 Hz	30 Hz	10 Hz	30 Hz
Final Velocity Heading	20 Hz	-	20 Hz	-	30 Hz	-
Delta	50 Hz	50 Hz	50 Hz	50 Hz	10 Hz	30 Hz
Peak Velocity	50 Hz	50 Hz	30 Hz	40 Hz	30 Hz	30 Hz
RMSE	40 Hz	40 Hz	50 Hz	40 Hz	30 Hz	30 Hz
Selected Filter	**50 Hz**	**50 Hz**	**50 Hz**	**50 Hz**	**30 Hz**	**30 Hz**

Table 5. Summary of linear regression coefficient estimates (Est.) and standard errors (S.E.) for peak resultant velocity (Peak V), peak resultant rotational velocity (Peak ω), change in translational velocity (ΔV), change in rotational velocity (Δω), initial translational velocity (V_0) and initial rotational velocity (ω_0). *P*-values correspond to student's *t*-test hypothesis testing in which the null hypotheses were that slope = 1, and intercept = 0.

		High Frame Rate			Intermediate Frame Rate			Low Frame Rate		
Parameter		Est.	S.E.	P	Est.	S.E.	P	Est.	S.E.	P
Peak V	**Int.**	0.058	0.087	0.514	0.063	0.118	0.600	0.463	0.197	0.034*
	Slope	0.994	0.016	0.692	1.002	0.022	0.946	1.035	0.038	0.377
Peak ω	**Int.**	4.345	2.489	0.745	3.072	4.105	0.467	9.279	3.225	0.012*
	Slope	0.839	0.078	0.060	0.916	0.140	0.556	0.763	0.116	0.060
ΔV	**Int.**	0.403	0.377	0.303	0.683	0.720	0.359	1.395	0.440	0.006*
	Slope	0.950	0.071	0.496	0.8551	0.1312	0.288	0.886	2.142	0.050*
Δω	**Int.**	2.437	1.999	0.243	0.029	2.968	0.992	6.700	3.686	0.091
	Slope	0.900	0.058	0.106	1.014	0.091	0.881	0.964	0.133	0.792
V_0	**Int.**	−0.036	0.054	0.514	0.081	0.166	0.632	0.030	0.282	0.918
	Slope	1.016	0.010	0.123	0.974	0.029	0.389	1.010	0.051	0.842
ω_0	**Int.**	0.241	0.312	0.454	0.162	0.237	0.505	0.527	0.401	0.210
	Slope	0.912	0.245	0.724	0.952	0.175	0.788	0.398	2.866	0.012*

*Result is statistically significant to a 0.05 significance level

could also be used to calculate the peak velocity and velocity change of the helmet during impact, which are more biomechanically relevant parameters. The average error associated with the video analysis was 9% for the change in translational helmet velocity and 17% for the change in rotational helmet velocity at intermediate frame rates (Figure 8(a)).

Previous studies have utilised broadcast video to estimate initial conditions for on-field head impacts (McIntosh et al., 2000; Pellman et al., 2003). A study by McIntosh et al. (2000) used video analysis of rugby matches to calculate pre-impact head velocities

Table 6. *P*-values calculated using a paired student's *t*-test between the errors associated with each of the video analysis frame rate scenarios.

		High	Intermediate			High	Intermediate
V_{max}	**Intermediate**	0.139		ω_{max}	**Intermediate**	0.336	
	Low	< 0.001*	0.038*		**Low**	0.250	0.482
ΔV	**Intermediate**	0.145		**Δω**	**Intermediate**	0.386	
	Low	0.002*	0.372		**Low**	0.029*	0.064
V_0	**Intermediate**	0.165		ω_0	**Intermediate**	0.409	
	Low	0.008*	0.075		**Low**	0.072	0.019*

Table 7. Tabulated data for motion capture (MC) and videogrammetry-derived kinematics for high, intermediate and low frame rate scenarios for ATD 1 for all 10 test configurations.

		ATD 1									
	Test	1	2	3	4	5	6	7	8	9	10
Peak Velocity (m/s)	MC	9.77	10.37	8.87	3.94	5.62	4.49	4.59	6.45	6.76	6.51
	High	9.70	10.35	8.83	3.57	6.09	4.30	4.46	6.48	6.88	6.55
	Intermediate	9.47	10.10	8.72	3.87	6.15	4.30	4.65	6.29	6.39	8.12
	Low	8.08	9.66	8.98	2.92	4.98	3.69	4.91	5.50	7.04	5.90
Peak Rotational Velocity (rad/s)	MC	52.55	37.66	35.35	17.19	30.92	20.07	15.25	40.38	26.72	33.61
	High	59.51	49.52	28.58	22.87	27.85	20.92	14.89	45.38	27.77	31.34
	Intermediate	40.37	42.48	29.02	18.24	21.69	23.35	19.58	49.21	31.67	34.00
	Low	62.49	34.08	31.21	19.97	12.60	19.23	11.13	34.61	26.80	27.09
Initial Velocity (m/s)	MC	6.96	6.87	6.89	0.02	0.03	4.35	4.50	6.20	6.24	6.35
	High	6.82	6.82	6.87	0.03	0.03	4.28	4.42	6.20	6.24	6.42
	Intermediate	6.77	6.92	6.73	0.03	0.07	4.24	4.29	6.18	6.22	7.25
	Low	6.98	6.63	7.63	0.02	0.83	3.69	4.59	5.50	5.79	5.90
Initial Rotational Velocity (rad/s)	MC	0.17	1.17	0.41	0.09	0.27	0.13	0.41	1.45	1.73	1.93
	High	0.89	1.53	0.09	0.21	0.55	0.21	0.90	1.70	2.22	0.94
	Intermediate	0.91	1.28	0.64	0.12	0.06	1.08	0.20	1.57	2.06	1.22
	Low	2.99	0.45	1.63	0.00	0.00	1.42	1.81	3.63	2.68	3.04
Delta-V (m/s)	MC	7.28	5.80	5.37	3.94	5.59	5.59	2.96	4.68	6.20	6.97
	High	7.00	5.74	5.31	3.54	6.06	5.32	2.70	5.03	5.34	7.02
	Intermediate	6.97	6.99	5.06	3.85	6.17	5.54	2.91	5.27	5.11	7.87
	Low	7.30	5.28	5.65	2.39	5.16	4.88	2.74	5.58	5.43	6.58
Delta-ω (rad/s)	MC	64.07	46.98	47.62	17.23	30.80	20.72	15.49	40.64	27.29	34.38
	High	69.35	54.51	45.34	23.17	27.10	21.04	15.17	45.15	28.62	30.70
	Intermediate	57.02	49.30	41.90	18.64	21.78	23.67	19.48	48.60	31.22	33.32
	Low	65.61	30.97	33.83	19.23	12.60	17.80	10.19	33.40	26.48	24.57

and estimated a 10% average error in their 2-D video analysis (McIntosh et al., 2000). Newman et al. (2005) attempted to quantify error in closing speed for the videogrammetry techniques used by Pellman et al. (2003). This error analysis involved only three tests and found that the error in resultant pre-impact velocity magnitude ranged from 1% to 11%. In the present study, videogrammetry was able to estimate the pre-impact translational velocity of the helmet with an average error of less than 5%. Neither Newman et al. (2005) nor McIntosh et al. (2000) quantified error associated with videogrammetry for any other kinematic parameter, such as heading angle, change in velocity or rotational velocity. Thanks to improvements over the last two decades in the resolution and frame rate of broadcast video, as well as advancements in video analysis theory and software, this study was able to quantify the helmet velocity over a longer time, in more degrees of freedom, and with greater accuracy than past work. This more complete data set increases this videogrammetry technique's utility for use in

Table 8. Tabulated data for motion capture (MC) and videogrammetry-derived kinematics for high, intermediate and low frame rate scenarios for ATD 2 for all 10 test configurations.

		ATD 2									
	Test	1	2	3	4	5	6	7	8	9	10
Peak Velocity (m/s)	MC	-	-	-	-	8.98	4.34	4.25	6.78	6.05	6.39
	High	-	-	-	-	8.99	4.15	4.12	6.20	6.12	6.18
	Intermediate	-	-	-	-	9.12	4.34	4.85	6.40	6.43	6.25
	Low	-	-	-	-	8.80	3.99	3.69	5.87	5.41	6.03
Peak Rotational Velocity (rad/s)	MC	-	-	-	-	19.78	23.76	9.96	20.53	35.44	33.98
	High	-	-	-	-	20.40	25.70	9.03	22.11	33.33	31.37
	Intermediate	-	-	-	-	18.73	24.08	8.17	19.96	30.93	29.72
	Low	-	-	-	-	17.33	21.94	9.41	20.54	29.29	21.60
Initial Velocity (m/s)	MC	-	-	-	-	8.59	3.98	4.02	5.81	5.86	5.88
	High	-	-	-	-	8.38	4.09	4.08	5.64	5.76	5.76
	Intermediate	-	-	-	-	8.62	3.93	3.93	5.92	6.11	6.21
	Low	-	-	-	-	8.80	3.99	3.69	5.81	5.41	5.98
Initial Rotational Velocity (rad/s)	MC	-	-	-	-	2.65	0.79	0.86	1.27	2.96	2.69
	High	-	-	-	-	1.99	0.55	1.10	1.58	2.60	0.71
	Intermediate	-	-	-	-	1.80	0.45	0.52	0.72	2.96	2.08
	Low	-	-	-	-	2.37	0.57	0.58	1.02	2.41	1.93
Delta-V (m/s)	MC	-	-	-	-	4.16	5.89	2.82	5.22	4.90	6.68
	High	-	-	-	-	3.81	5.49	2.94	5.52	4.26	6.46
	Intermediate	-	-	-	-	4.07	5.24	4.26	4.96	4.48	6.78
	Low	-	-	-	-	3.62	5.43	2.01	4.50	3.67	6.03
Delta-ω (rad/s)	MC	-	-	-	-	19.94	22.57	9.01	19.90	35.86	34.84
	High	-	-	-	-	20.05	25.22	8.03	21.51	32.10	31.06
	Intermediate	-	-	-	-	19.16	23.59	7.64	19.57	31.53	29.51
	Low	-	-	-	-	18.38	21.61	9.19	19.96	28.68	21.70

Note: ATD2 was not involved in tests 1–3 and the data acquisition for ATD2 failed to trigger for test 4, so no data is reported for those tests.

developing forward dynamics models for estimating the forces and moments applied to the helmet, which may lead to concussion.

The estimated errors in the current videogrammetry technique were comparable to or lower than errors previously reported in similar studies. In a study in which the head kinematics of pedestrian dummies struck by vehicle bucks (mock-up of automobiles for testing) at 40 kph were determined using model-based image-matching, Tierney et al. (2017) reported RMSEs between 0.4–1.3 m/s and 3.5–5.4 rad/s for the linear and angular velocities, respectively. The corresponding RMSEs in the present study ranged from 0.2–0.9 m/s and 2.0–6.0 rad/s for the high frame rate case. These error estimates are in good agreement, considering that Tierney et al. (2017) analysed 100 fps video and we analysed 240 fps video.

One important limitation of this study is that the videogrammetry tracked helmet motion, not head motion. Relative translational and rotational motion between the head and helmet have been noted during impact testing, which limits the effectiveness of sensors installed in the helmet and the ability of helmet tracking to deduce information about head kinematics (Beckwith, Greenwald, & Chu, 2012; Jadischke et al., 2013). Nevertheless, quantifying helmet motion provides useful information about the severity of the head impact. The ability to accurately measure closing velocities of players and resulting changes in velocity for events where sensors have not been used provides a unique opportunity to retroactively characterise how helmets are loaded in the on-field environment.

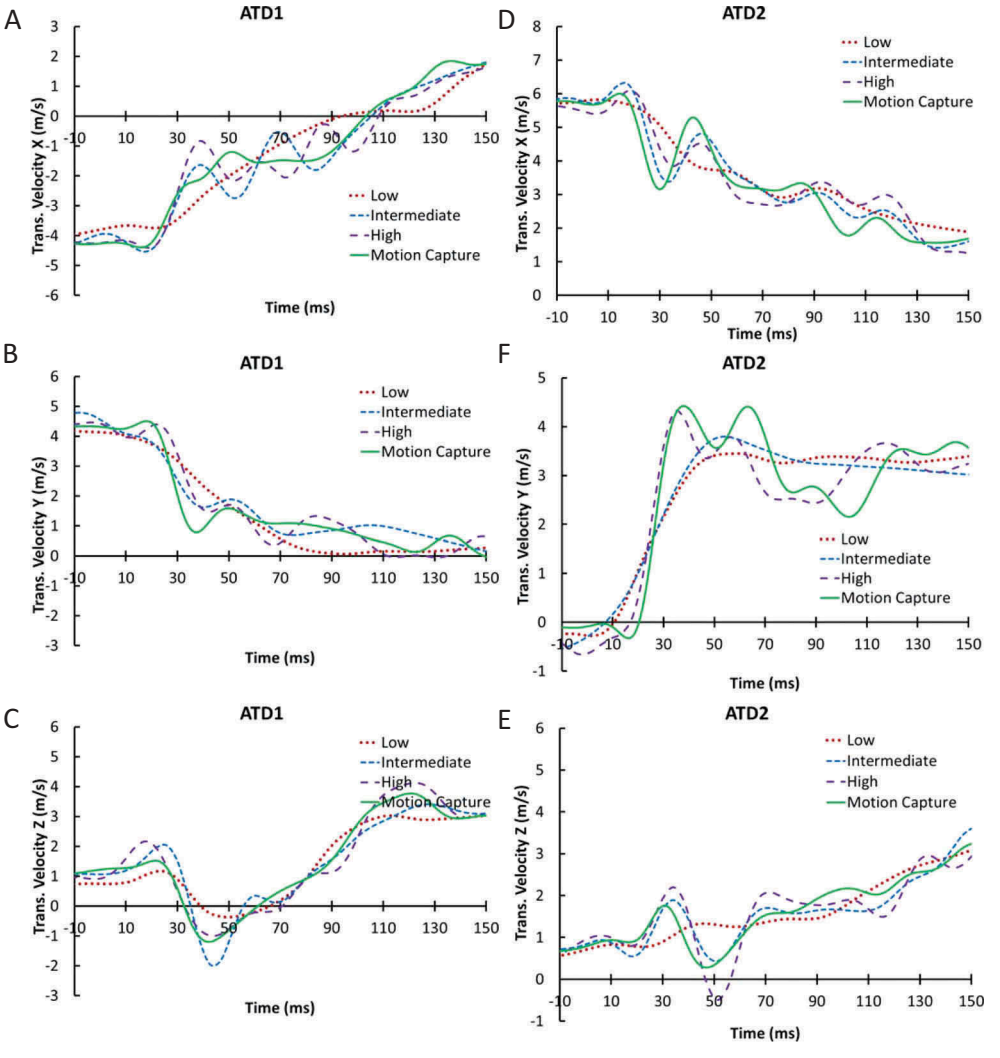

Figure 9. Comparison of translational velocity components from videogrammetry and Vicon™ for configuration 8 for both ATD1 (A-C) and ATD2 (D-F) helmets.

Conclusion

In summary, the videogrammetry technique was found to be more accurate at measuring initial, pre-impact velocities than change in velocities during the impact. Further, the accuracy of the measured change in velocity was found to be greater for cases for which at least one camera view had a frame rate of 240 Hz compared with cases for which both camera views had frame rates of 60 fps. If one camera view had high frame rate footage (240 images/s), then the change in translational helmet velocity could be measured with an overall error of 0.4 m/s (9%) and the change in rotational helmet velocity could be measured with an overall error of 3 rad/s (17%). This study supports the use of videogrammetry to measure helmet velocity before, during and after impact

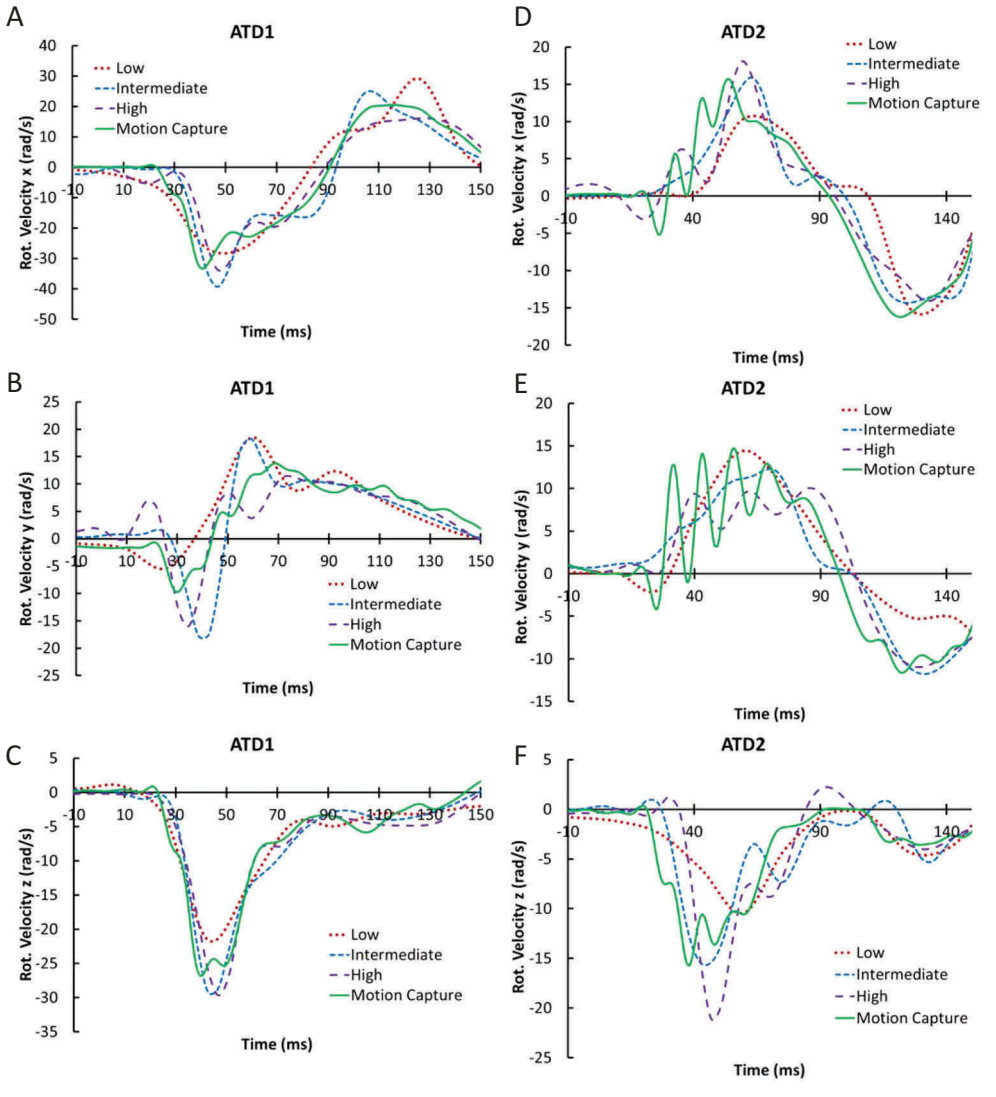

Figure 10. Comparison of rotational velocity components from videogrammetry and Vicon™ for configuration 8 for both ATD1 (A-C) and ATD2 (D-F) helmets.

in all six degrees of freedom, provided that sufficiently high-quality footage is available with at least one view shot at a high frame rate (240 images/s or greater). By applying the videogrammetric techniques described in this paper to broadcast video of concussion-causing impacts in NFL games, we hope to generate naturalistic data that will inform decisions about future helmet testing protocols, establish input conditions for dummy reconstructions of actual game impacts, and improve our understanding of the impact conditions that lead to concussion.

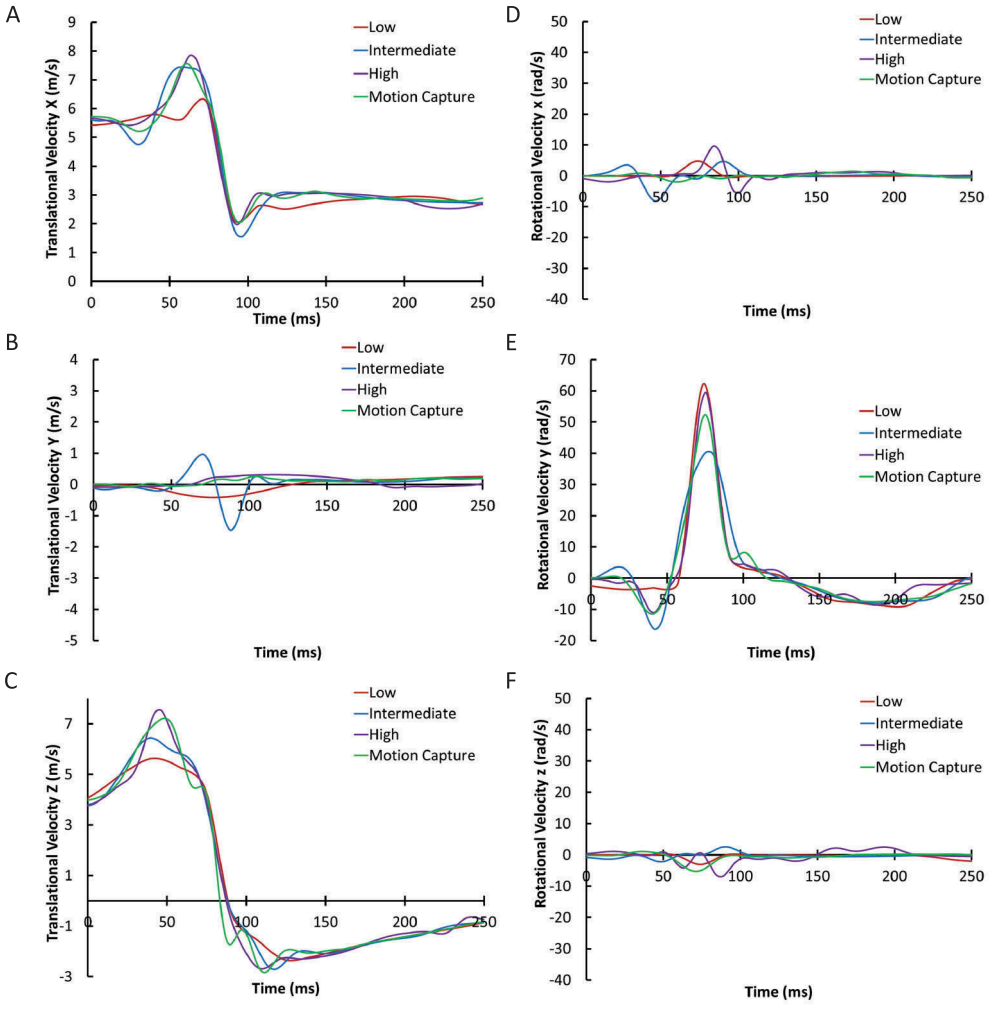

Figure 11. Comparison of translational (A-C) and rotational (D-F) velocity components from videogrammetry and Vicon™ for configuration 1 helmet-to-ground test. The pelvis contacted the ground at 0 ms and helmet-to-ground contact occurred at 80 ms.

Acknowledgments

The research presented in this paper was made possible by a grant from Football Research, Inc. (FRI). The authors acknowledge the contributions of the National Football League Players Association (NFLPA). The views expressed are solely those of the authors and do not represent those of FRI or any of its affiliates or funding sources. The authors would also like to acknowledge McCarthy Engineering Inc., Biocore LLC, Kineticorp, and the University of Virginia Centre for Applied Biomechanics for their technical and equipment support.

Disclosure statement

No potential conflict of interest was reported by the authors.

References

Beckwith, J., Greenwald, R., & Chu, J. (2012). Measuring head kinematics in football: Correlation between the head impact telemetry system and hybrid III headform. *Annals of Biomedical Engineering*, *40*, 237–248. doi:10.1007/s10439-011-0422-2

Camarillo, D. B., Shull, P. B., Mattson, J., Shultz, R., & Garza, D. (2013). An instrumented mouthguard for measuring linear and angular head impact kinematics in American football. *Annals of Biomedical Engineering*, *41*, 1939–1949. doi:10.1007/s10439-013-0801-y

Gehre, C., Gades, H., & Wernicke, P. (2009). Objective rating of signals using test and simulation responses. In *Proceedings: International Technical Conference on the Enhanced Safety of Vehicles* (Vol. 2009). National Highway Traffic Safety Administration.

Jadischke, R., Viano, D. C., Dau, N., King, A. I., & McCarthy, J. (2013). On the accuracy of the head impact telemetry (HIT) system used in football helmets. *Journal of Biomechanics*, *46*, 2310–2315. doi:10.1016/j.jbiomech.2013.08.006

Jadischke, R., Viano, D. C., McCarthy, J., & King, A. I. (2016). The effects of helmet weight on hybrid III head and neck responses by comparing unhelmeted and helmeted impacts. *Journal of Biomechanical Engineering*, *138*, 1–10. doi:10.1115/1.4032997

Koga, H., Nakamae, A., Shima, Y., Iwasa, J., Myklebust, G., Engebretsen, L., … Krosshaug, T. (2010). Mechanisms for noncontact anterior cruciate ligament injuries knee joint kinematics in 10 injury situations from female team handball and basketball. *American Journal of Sports Medicine*, *38*, 2218–2225. doi:10.1177/0363546510373570

Lessley, D., Shaw, G., Riley, P., Forman, J., & Crandall, J. (2011). Assessment and validation of a methodology for measuring anatomical kinematics of restrained occupants during motor vehicle collisions. *Journal of Biosensors and Bioelectronics*, *S1*, 002. doi:10.4172/2155-6210.S1-002

McIntosh, A. S., McCrory, P., & Comerford, J. (2000). The dynamics of concussive head impacts in rugby and Australian rules football. *Medicine and Science in Sports and Exercise*, *32*, 1980–1984. doi: 10.1097/00005768-200012000-00002

National Operating Committee on Standards for Athletic Equipment. (2015). *Standard method of impact test and performance requirements for football faceguards* (Report No. NOCSAE DOC 087-12m15a). National Operating Committee on Standards for Athletic Equipment website. Retrieved from http://nocsae.org/wp-content/files_mf/1451498030ND08712m15aFootballFGStandard.pdf

Neale, W. T., Hessel, D., & Koch, D. (2016). *Determining position and speed through pixel tracking and 2D coordinate transformation in a 3D environment* (Technical Paper No. 2016-01-1478). SAE website. Retrieved from http://papers.sae.org/2016-01-1478/

Neale, W. T., Hessel, D., & Terpstra, T. (2011). *Photogrammetric measurement error associated with lens distortion* (Technical Paper No 2011-01-0286). SAE website. Retrieved from http://papers.sae.org/2011-01-0286/

Newman, J. A., Beusenberg, M. C., Shewchenko, N., Withnall, C., & Fournier, E. (2005). Verification of biomechanical methods employed in a comprehensive study of mild traumatic brain injury and the effectiveness of American football helmets. *Journal of Biomechanics*, *38*, 1469–1481. doi:10.1016/j.jbiomech.2004.06.025

Oeur, R. A., Karton, C., Post, A., Rousseau, P., Hoshizaki, T. B., Marshall, S., … Gilchrist, M. D. (2015). A comparison of head dynamic response and brain tissue stress and strain using accident reconstructions for concussion, concussion with persistent postconcussive symptoms, and subdural hematoma. *Journal of Neurosurgery*, *123*, 415–422. doi:10.3171/2014.10.JNS14440

Pellman, E. J., Viano, D. C., Tucker, A. M., Casson, I. R., & Waeckerle, J. F. (2003). Concussion in professional football: Reconstruction of game impacts and injuries. *Neurosurgery*, *53*, 799–814. doi:10.1093/neurosurgery/53.3.799

Rowson, S., Beckwith, J. G., Chu, J. J., Leonard, D. S., Greenwald, R. M., & Duma, S. M. (2011). A six degree of freedom head acceleration measurement device for use in football. *Journal of Applied Biomechanics*, *27*, 8–14. doi:10.1123/jab.27.1.8

Rowson, S., & Duma, S. M. (2013). Brain injury prediction: Assessing the combined probability of concussion using linear and rotational head acceleration. *Annals of Biomedical Engineering*, *41*, 873–882. doi:10.1007/s10439-012-0731-0

Siegmund, G. P., Guskiewicz, K. M., Marshall, S. W., DeMarco, A. L., & Bonin, S. J. (2016). Laboratory validation of two wearable sensor systems for measuring head impact severity in football players. *Annals of Biomedical Engineering*, *44*, 1257–1274. doi:10.1007/s10439-015-1420-6

Society of Automotive Engineers. (1995). *Instrumentation for impact tests* (Report No. SAE J211). SAE website. Retrieved from https://www.sae.org/standards/content/j211/1_199503/

Tierney, G. J., Joodaki, H., Krosshaug, T., Forman, J. L., Crandall, J. R., & Simms, C. K. (2017). Assessment of model-based image-matching for future reconstruction of unhelmeted sport head impact kinematics. *Sports Biomechanics*, *17*, 33–47. doi:10.1080/14763141.2016.1271905

Viano, D. C., Withnall, C., & Halstead, D. (2012). Impact performance of modern football helmets. *Annals of Biomedical Engineering*, *40*, 160–174. doi:10.1007/s10439-011-0384-4

Wu, L. C., Zarnescu, L., Nangia, V., Cam, B., & Camarillo, D. B. (2014). A head impact detection system using SVM classification and proximity sensing in an instrumented mouthguard. *IEEE Transactions on Biomedical Engineering*, *61*, 2659–2668. doi:10.1109/TBME.2014.2320153